RSC Sustainability



PERSPECTIVE

View Article Online
View Journal | View Issue



Cite this: RSC Sustainability, 2023, 1, 224

Perspectives in growth production trade-off in microbial bioproduction

Deepanwita Banerjee and Aindrila Mukhopadhyay ab

Metabolic engineering of microbial systems and conversion routes can provide robust platforms for the production of bulk commodities for food, materials and fuel targets. For products in this range, the maximum conversion of starting materials and stable phenotypes in a bioreactor are vital for an economically viable process. Strain engineering approaches to improve the conversion efficiency and reduce the phenotypic variability have witnessed significant development in the past decade. Herein, we review several of the main categories of these approaches including growth coupling, growth decoupling, regulatory control and use of non-metabolic cellular functions. We discuss these topics in the context of microbial host physiology and its impact in the selection of the most effective approach. We also discuss the importance of growth medium optimization and studies using bioreactors in delineating a bioproduction system that is most likely to provide stable conversion over a longer period.

Received 1st October 2022 Accepted 24th November 2022

DOI: 10.1039/d2su00066k

rsc.li/rscsus

Sustainability spotlight

In 2019, the renewable energy consumption increased but its share in the total energy consumption was 17.7%, which is only 1.6% higher than that in 2010. In 2020, governments spent \$375 billion on subsidies for fossil fuels. Subsequently, in 2021, the fuel-related emissions were at their highest and eliminated the pandemic-related reduction seen in 2020. These challenges can be addressed through the faster scale-up of renewable fuels and commodity chemicals. The sustainable production of many previously petrochemically derived chemicals can be realized *via* microbial production using renewable starting materials, but for success, this requires the maximum conversion and balancing cultivation with final product formation in the process. This is in alignment with the UN Sustainable Development Goals including affordable and clean energy, responsible consumption and production, and climate action.

Introduction

Biotechnological application is no longer limited to the pharmaceutical industry and fine chemicals but is also widely applied for the production of food, fuel and other commodity chemicals. After optimization of the biosynthetic pathway, the production yield required for these commodities remains high. and therefore maximum conversion of the starting materials is necessary for economical, sustainable production of these bulk chemicals. To achieve this, several engineering strategies can be employed, which are both rational and computationally driven. In principle, all these approaches can be implemented for all microbial systems and target products, but in practice, their experimental implementation is conducted in a small set of model hosts (e.g., E. coli and S. cerevisiae) and targets. Furthermore, in the case of systems that have been experimentally vetted, few have been scaled up. Consequently, these microbial bioconversion methods for commodity chemical production are still far from being host-, product-, substrate-, and scale-agnostic.

A key parameter to consider in de-risking microbial production is that growth and bioproduction are linked. Although robust growth is required for efficient production, both growth and production also utilize the same pool of starting materials, creating a trade-off (Fig. 1A). Bioproduction mainly falls into three categories (Fig. 1B) that utilize a natural phenotype for accumulating a bioproduct. The first is secondary metabolism, rerouting a small amount of cellular intermediates to make a final product that has specialized use. Most engineering pathways (including heterologous pathways) fall in this category. The second is in the form of storage molecules such as polyhydroxyalkanoates (PHA), lipids, and fatty acids. The third is redox balancing by-product accumulation such as CO₂, ethanol, and organic acids. Ethanol is one of the best bioconversion examples that works in exactly the desired conditions, i.e., high sugar load and low O2. Moving forward, mixed carbon co-feed and carbon (C) and nitrogen (N)-centric genome-scale metabolic representations hold immense potential in addressing the trade-off for the bulk production of commodity chemicals.

For the maximum conversion and ideal hosts, products, substrates, and scale agnostic bioconversion success of any type (Fig. 1C), the trade-off introduced through strain/host engineering can be addressed with the right combination of host

^aBiological Systems and Engineering, Lawrence Berkeley National Laboratory, 1 Cyclotron Road, Berkeley, CA 94720, USA. E-mail: amukhopadhyay@lbl.gov ^bJoint BioEnergy Institute, Emeryville, CA, 94608, USA

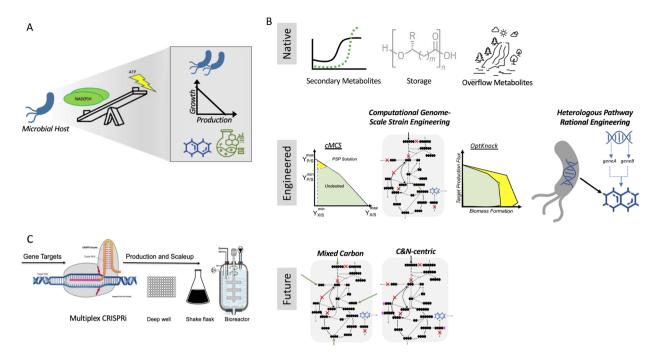


Fig. 1 Role of growth production trade-off in microbial conversion for the production of bulk chemicals. (A) Growth production trade-off in a microbial host. (B) Approaches to better utilize the trade-off towards bioconversion to commodity chemicals. (C) Overall goal of a successful bioconversion process

and product, and thus these methods need to be more widely applied.

Growth coupling (GC)

The translation of the majority of proof of principles tested on the lab scale to industrial production platforms is very unpredictable, and thus most systems have not been tested.2 Among the various challenges, one major bottleneck is that if the production is independent of microbial growth, growth inhibition due to the expression of a burdensome pathway or production of an inhibitory compound can cause engineered strains to drift away from their optimal production phenotype due to its selective advantage. Thus, to address this challenge, coupling growth with production is a powerful strategy for evolving strains to maintain high titers, rates, and yields (TRY). Three main definitions of growth coupling have been widely used in the metabolic engineering for microbial conversion. First, the most popular approach is optimal production at the optimal growth rates (*weak coupling*), where the earliest example includes the use of Optknock for the production of lactate in E. coli³ and one popular example is Optknock-based strain engineering for the production of 1,4 BDO in E. coli4. Second, when production is coupled with a driving force such as ATP production or NADPH or NADH cofactor balancing. These coupling strategies have been used for the production of short chain primary alcohols (1-butanol, isobutanol, and 2-methylbutanol) in Escherichia coli⁵ and Synechococcus sp.^{6,7} as well as for 3-hydroxypropionic acid production in Saccharomyces cerevisiae.8 Third, when metabolite production is essential for growth, which is also termed strong coupling or obligatory

production. This type of strong growth coupling is found in nature, where examples include ethanol under fermentative state (e.g., S. cerevisiae), carbon dioxide during microbial aerobic growth and acetate in acetogenic bacteria. An iterative implementation of computed constrained Minimal Cut Sets (cMCSs) using a modified central metabolic model of E. coli for itaconate production9 resulted in significantly high titers (32 g L⁻¹) and itaconate yield (0.77 mol mol⁻¹ glucose) with negligible by-product (pyruvate) although it required glutamate supplementation in the fed batch cultivation. Recent advancement in cMCS computation at the genome-scale 10,11 led to the engineering of Pseudomonas putida for the production of indigoidine, a bipyridyl molecule, using a product-substrate-pairing (PSP) approach (Fig. 2).12 This study reported the highest indigoidine titer (26 g L⁻¹) to date at that time, which remains the highest using glucose minimal media and made more of indigoidine during glucose feeding, i.e., the indigoidine production was in the growth phase. In general, these GC prediction strategies assume the best or optimal growth conditions for the host, and therefore GC engineering when followed by adaptive laboratory evolution (ALE) should improve the production phenotype given that growth is hard-wired to production and ALE will trace the path for better growth in the fitness landscape. In the case of non-conventional microbial systems, it may be a challenge to determine the best growth cultivation condition (discussed later in this review). This bottleneck can be addressed using medium optimization methods such as design of experiment (DOE) or high throughput (HT) phenotypic profiling in combination with machine learning.

Although growth-coupled strategies are promising, sometimes their direct implementation may result in auxotrophy. For

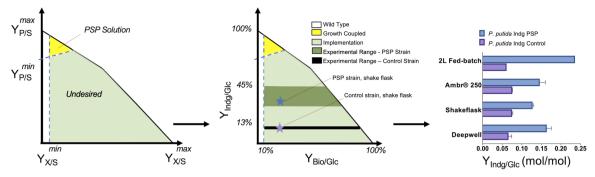


Fig. 2 Product substrate pairing (PSP) approach for the growth-coupled microbial conversion of glucose (Glc) to indigoidine (Indg), adapted from Banerjee et al.

example, OptGene-based *S. cerevisiae* strain engineering for the production of succinic acid resulted in glycine auxotrophy. ¹³ Upon ALE the resulting strain had significant improvement in succinate titre (0.9 g L⁻¹) and growth rates, but the yields were still low (0.05 g g⁻¹ of glucose or 0.43 *versus* 0.69 g g⁻¹ of biomass) due to the trade-off between growth and production. This trade-off due to competition for the same resources also resulted in significant dependence on available oxygen when growth-coupled strain engineering in *E. coli* was performed using elementary mode analysis for ethanol production. ¹⁴ Recently, growth-coupled production examples have been comprehensively reviewed. ^{15,16} Growth-coupled schemes are also being investigated for *in vivo* biohalogenation ¹⁷ as well as protein production. ¹⁸

Decoupling growth and production (DC)

To address the trade-off between growth and production, the separation of the two phases during any microbial process, i.e., growth phase and production phase, has been shown to be promising. This avoids the metabolic burden of the production pathway during the growth phase and helps in the allocation of all metabolic resources to the synthesis of the product during the production phase. These approaches for microbial conversion have been widely used for the utilization of non-canonical carbon sources such as glycerol,19 xylose,20 protocatechuate,21 hydrocinnamic acids,22 and toxic products such as 1,2-indandiol production in Rhodococcus sp.23 The transition from one phase to another is induced by several different strategies. Examples include glucose starvation and carbon source switching for the production of PHB in E. coli in rich and minimal media,24 nitrogen starvation for fatty alcohol production in E. coli,25 phosphate limitation for linalool production in Pantoea ananatis,26 oxygen supply limitation,27 biotin limitation for proline production in Corynebacterium glutamicum,28 pH control for propionic acid production in Propionibacterium jensenii19 and temperature shift29 to regulate isocitrate dehydrogenase activity to increase itaconate production in E. coli. 30 Extreme examples are growth in one carbon source and conversion of a different source to the product21,23 or use of whole cells as biocatalysts for the production of acetoin, gamma-amino-butyric acid (GABA) and ϵ -caprolactone using engineered $E.~coli.^{31-33}$ The earliest example of growth decoupling to separate growth from production using stationary phase production was the production of trans-(1R,2R)-indandiol in Rhodococcus sp. $I24.^{23}$ Examples of co-production include a growth-decoupled fed-batch production process, which resulted in the formation of about 11 g L $^{-1}$ α -ketoglutarate and succinate from xylose in $C.~glutamicum.^{20}$ Advancement in computational implementations for identifying a range of operating points within a feasible solution space has also been reported. 34

A major challenge of decoupled microbial conversions that use constitutive production pathways is that during the growth phase, there may be a phenotypic drift due to suboptimal growth or toxicity and low-producing variants with fitness advantages may overtake the population in the bioconversion process. One approach to address this challenge is the native auto-induction method for bioconversion. Auto-induction is based on the lac operon regulatory function during diauxic growth in the presence of multiple carbon sources such as glucose, glycerol, and lactose.35 Although the control of these natural circuits is well characterized in E. coli, catabolite repression and preferential carbon source utilization in "rising star" hosts still need to be elucidated for bioproduction purposes. In this case, tighter control through synthetic feedback or feed-forward loops may help devise better solutions to overcome these trade-offs.

Synthetic circuits for dynamic control (feed-back/feed-forward loops)

Advances in gene editing technologies^{36,37} have made the design of gene circuits easier for accurate dynamic control to balance the existing trade-off between growth and bioconversion. One of the earliest examples is a two-layered circuit design that decoupled growth and production and utilized product-addicted promoters to amplify production in *E. coli.*²² This lowered the metabolic stress and increased the growth rate and vanillic acid productivity. An example of GC together with dynamic control resulted in a high naringenin-producing *E. coli* strain

 $(523.7 \pm 51.8 \text{ mg L}^{-1})$ with 20% increase in cell growth compared to the control strain.38 An example of this dynamic control is the switch between growth and production phase for GABA production in C. glutamicum, which produced 45.6 g L^{-1} of GABA with a yield of 0.4 g g⁻¹ glycerol.³⁹ Cell density based quorum-sensing circuits in *E. coli* resulted in 520 \pm 7 mg L⁻¹ salicylic acid, which is a 1.8-fold improvement compared to the control strain.40 Nitrogen limitation-driven dynamic control for the production of itaconate⁴¹ was extended to produce itaconate at 1.4 g L⁻¹ in *P. putida* from deconstructed lignin. Another example of dynamic control of pH has been reported for the production of lycopene in E. coli. 42 On-off switches, which have been also used by genetic engineers, are inversion promoter regions based on recombination events.

Gene circuits for synthetic addiction have been successfully developed in model organisms but can be context specific. Metabolite-responsive transcription factor-based biosensors have been the most successful thus far and hold immense potential but their dynamic range may be growth dependent and vary under different media conditions and growth environments. Recently, it was reported that the dynamic range of aTc-TetR and IPTG-LacI sensors has positive correlations with the cell growth rate, whereas the FA-FadR biosensor has a negative correlation with the cell growth rates when tested for several carbon sources in minimal media condition, confirming the trade-off between the dynamic range and growth condition.43 However, optimization is challenging when using a synthetic feed, given that only narrow sweet spots exist. These gene circuits are still not scalable across products and formats due to several challenges including their narrow dynamic range, linearity, and signal to noise ratio. A successful alternative was the design of genetically stable circuits or "landing pads" in the E. coli genome, where the expression level is high,44 and creation of insulators using the NOR gate logic. Recently, this has been extended to S. cerevisiae and Bacteroides thetaiotaomicron. 45 Computational workflows are also being developed for multiobjective optimization for the trade-offs associated with biosensor development. 46,47 Another challenge that remains is the enrichment of producers versus escapers or non-producers, as reported for baker's yeast.48 Recent examples of biosensorbased dynamic regulation have been reviewed elsewhere.49

Recently, optogenetic tools have also been utilized for the production of various value-added products such as lactic acid, isobutanol, and shikimic acid. Zhao et al. 50 produced 8.49 g L⁻¹ of isobutanol in S. cerevisiae using OptoEXP- and OptoINVRTbased control of EL222 transcriptional activator for metabolic switching to the production phase. Subsequently, a further optimized version, i.e., OptoAMP-based control of LDH, was reported for the production of lactic acid 6 g L^{-1} in S. cerevisiae even at low light intensities.⁵¹ In another study, optogenetic tools were developed using the TetR system together with the tobacco etch virus protease (TEVp) for the production of shikimic acid in E. coli at 35 g L⁻¹ using glucose minimal media.⁵² The major bottlenecks with optogenetic tools include the limited number of photo-switchable proteins, restricted implementation in popular industrial hosts, insufficient and heterogeneous lighting at high cell density in large-scale

bioreactors and cost associated with specifically designed industrial-scale light-bioreactors (up to 5000-10000 L) for the production of commodity chemicals. Another major challenge is the metabolic burden associated with the cellular resource allocation to build the multiple proteins and cofactors (FMN, NADH, and NADPH) required for the functioning of these optogenetic systems. Examples of various optogenetic tools have been recently reviewed elsewhere.53

Multi-substrate-based synthetic circuits for metabolic control of bioconversion processes have been reported54 but are still to be routinely implemented for production control. These synthetic genetic control systems should at least include substrate-induced transitions from the growth to production phase (decoupled production). Thus far, some progress in this direction has been reported for S. cerevisiae⁵⁵ and E. coli²⁴ but there has not been much progress in growth-coupled bioproduction strategies to the best of our knowledge. An aspect to consider in dynamic control circuits is the maintenance of the phenotype in a variable or heterogeneous environment. Specifically, for use in larger-scale production, the circuit must retain a high signal to noise ratio and have minimal interference from any crosstalk. Given that it is challenging to predict these issues a priori, implementation and examination of these systems in larger-scale fed-batch mode with industrially relevant feed sources are necessary.

Medium optimization for scalable bioconversion systems

Another critical factor in the growth-production trade-off, and consequently in the advancement and scaleup of bioconversion systems is the medium composition and its role in engineered strain cultivation during the bioconversion process. Examples of medium optimization to improve productivity are both essential and well-reported. In this section, we review medium optimization in the context of growth-production trade-off, such as the use of mixed carbon and the impact of carbon: nitrogen (C/N) ratios.

Well-defined media with minimal nutrient supplementation are ideal from a techno-economic perspective; however, the use of resources coming from poorly utilized but abundant feedstocks is also necessary, both aiming towards a carbon-negative bioconversion process. Furthermore, successful bioconversion for commodity chemicals is measured by titer, rates, and yields (TRY), which is challenging to quantify in rich media or in undefined media such as plant biomass-derived feedstocks. These factors play a role in the use of growth-pairing strategies. To date, growth-coupled strategies have been examined for only a single C source. Mixed C-sources have been shown with DC strategies but it is necessary to further engineer strategies that account for more than one carbon source to address the growth productivity trade-off. An example towards advanced bioconversion systems using carbon negative feedstocks reported that a cofeed of CO2 and glucose enhanced acetogenesis in Moorella thermoacetica, whereas gluconate and acetate cofeed enhanced fatty acid production in Yarrowia lipolytica under fed-batch

condition.⁵⁶ Another example involved DC engineering of a heterologous Weimberg pathway bypass in the itaconate producer E. coli Δicd strain, which led to a high titer of 20 g L⁻¹ itaconate and ~65% of maximum theoretical yield (glycerol) using a cofeed of glycerol and xylose.⁵⁷ Given that GC strategies are hard wired to the carbon source, it will be interesting to see how the production phenotype performs when multiple carbon sources or a nutrient-rich medium such as plant biomassderived hydrolysate is used as the carbon stream for bioconversion to commodity chemicals using such engineered strains. Carbon sources that are incompatible with growth-coupling engineering may reduce the TRY, whereas compatible carbon sources may have a synergistic effect on the product yield (for example, growth coupling with glucose is synergistic with galactose but may be incompatible with aromatic substrates). 12 The GC algorithm used in the PSP pipeline is customizable for co-feed substrate utilization but it has not been experimentally implemented thus far. To truly understand the growth versus production Pareto front, accurate measurements of TRY are required, but remain a challenge to obtain routinely. In the case of DC strategies, glucose is a well-studied and preferred carbon source, whereas the bioconversion medium components such as nitrogen, oxygen, phosphate, temperature and other limitations may have far more complex relationships to have tight transitions between the two phases and may not scale successfully to industry relevant bioreactor cultivation conditions. For example, biotin limitation under the fed-batch regime induced glutamate secretion as a by-product in C. glutamicum.28 In another extreme example, only 4 out of 16 phosphate-regulated promoters tested in E. coli scaled successfully to the bioreactor condition (ugpB, yibD, phoA, and phoB promoters).58

Finally, instead of implementing GC with multiple substrates in the same strain, a viable near-future alternative is a one-pot synthetic microbial community of GC-engineered strains for the division of labor for the bioconversion of specific substrates efficiently. A similar division of labor has been used to reduce the metabolic burden in a P. putida and S. cerevisiae consortium to produce 295.7 mg L⁻¹ mcl-PHA titer.⁵⁹ Recently, a synthetic microbial consortium of P. putida and E. coli was reported, where substrate utilization and production were decoupled in the two strains, which resulted in 1.32 g L⁻¹ of mcl-PHA from 20 g L^{-1} of a glucose-xylose mixture (1:1).60 Computational dynamic modeling has also been used to study the trade-off between productivity and efficiency of substrate utilization in a synthetic consortium of E. coli strains, with one producing a heterologous protein together with a second E. coli strain engineered to scavenge acetate.61

Nitrogen is another major constraint that is usually overlooked in various engineering strategies. The optimization of the C/N ratio in bioprocess optimization is required to identify the best bioconversion cultivation condition $^{62-64}$ or supplementation of large amounts of nitrogen sources (e.g., 1 g L $^{-1}$ or higher supplementation in production medium during scale-up). Firstly, nitrogen has been extensively used for metabolic engineering purposes to address the growth *versus* production trade-off of storage metabolites that are triggered by N starvation such as PHA production in *P. putida* strains. 65,66 Secondly,

research is shifting towards "greener" non-conventional carbon feedstocks containing aromatics, furfurals, etc., which follow different catabolic routes and regulatory mechanisms to generate energy and maintain cellular biomass (not the conventional glycolysis \rightarrow TCA \rightarrow oxidative phosphorylation). Aromatic catabolism is very different from traditional sugar glycolytic pathways. Conventional knowledge is that when glucose, fatty acids, or some amino acids are utilized as a carbon source under aerobic conditions, the C/N ratio sensing metabolic node is alpha-ketoglutarate (AKG).67 However, this may not be true for aromatics or other carbon sources. C and Ncentric context-specific genome-scale metabolic models (GSM) and 13C- and 15N-labeled metabolic flux analysis (MFA) under a range of different conditions will advance the GSM closer to Cand N-relevant experimental conditions. Further, as is often the case with the carbon source, a certain N source can also be more suitable for a host or a conversion process, and a given medium formulation may not hold true if the host, pathway or culture format is changed for the same bioconversion system. 63,68

Given that the final products span a greater range of targets, we now encounter products that are metabolized or degraded by the host microbe. Product degradation or catabolism also indirectly related to growth-production pairing and medium amendments has been used to prevent product catabolism. For example, in isoprenol production in *P. putida*, it was found that the natural catabolism of isoprenol occurs only after the consumption of glucose (Xi *et al.*, *2 in their review). In general, metabolically versatile hosts such as *P. putida* have catabolic pathways for many final products or precursors. This can also be addressed *via* the deletion of the catabolic route when known. 69,70 However, to the best of our knowledge, there are not enough systematic studies on the effect of media components on highly engineered strains that are tailored for bioconversion on a large scale.

Medium optimization is an integral part of process optimization for any bioconversion process.71-73 From a synthetic biology perspective, metabolic pathways and host engineering research must also incorporate the knowledge of the medium components on the metabolism being engineered. It is understood that during scale-up from the lab to industrial level, medium and process optimization plays a significant role in research and development. However, even at the lab-scale design, requirements of media formulations can be incorporated into strain design. In the case of strains devoid of hierarchical substrate uptake and utilization (using modification in master regulators, e.g., delta crc), accessory machinery (e.g., EM42 strain) allows rewiring the host metabolism as well as cell physiology, and thus the trade-off is now substantially altered relative to the basal strain. The C/N ratio for the new strain designs will be different, and therefore requires reintegration in the form of a medium optimization module. However, despite the essentiality of medium optimization, it remains ad hoc in the literature⁷³ and few examples of high throughput datadriven medium optimization exist.74,75 One can anticipate that with improvements in automation and data-driven approaches and the ability to examine configurations in high throughput (e.g., via microfluidics76), this aspect will also witness a lot of

Table 1 All examples discussed in this review $^{\!\varepsilon}$

	Product	TRY^a	Host	Media	Reference
Growth coupled					
1	Lactic acid b	$1.75~{ m g}~{ m L}^{-1}$	E. coli	M9 glucose	Fong et al., 2005 (ref. 3)
2	$1,4~\mathrm{BDO}^b$	$18~{ m gL}^{-1}$	E. coli	M9 glucose	Yim <i>et al.</i> , 2011 (ref. 4)
3	$1 ext{-Butanol}^b$	$30~{ m g~L^{-1}}, 70\%~{ m yield}, 0.18~{ m g~L^{-1}}~{ m h^{-1}}$	E. coli	Glucose	Shen <i>et al.</i> , 2011 (ref. 5)
4	1 -Butanol b	$29.9~{ m mg~L}^{-1}$	Synechococcus	BG-11	Lan and Liao, 2012 (ref. 6)
,			sp.	-	
2	2-Methyl-1-butanol, isobutanol	$1/1~{ m mg}~{ m L}^{-}$ and $181~{ m mg}~{ m L}^{-}$	Synechococcus sp.	MAD media	Furdy <i>et al.</i> , 2022 (ref. 7)
9	3-Hydroxypropionic	$463 \mathrm{~mg~L^{-1}}$	S. cerevisiae	Glucose	Chen et al., 2014 (ref. 8)
	acid^b				
7	Itaconate ^b	$32~{\rm g}~{\rm L}^{-1}, 0.68~{\rm mol}~{\rm mol}^{-1}~{\rm and}~0.45~{\rm g}~{\rm L}^{-1}$ h ⁻¹	E. coli	Glucose + glutamic acid	Harder <i>et al.</i> , 2016 (ref. 9)
0	Indigoidine	11 26 ∝ 1 −1	D mutida	Mo whoose	Baneriee of al 2020 (ref 12)
0 0	Succinic acid ^{b}	$0.9 \text{ o } 1.^{-1} \cdot 0.05 \text{ o } 9^{-1}$	S. cerevisiae	Glucose + Glv/Thr	Dancijec et $ai.$, 2020 (121. 12) Otero et $al.$, 2013 (ref. 13)
10	$Ethanol^b$	$0.44~\mathrm{gg^{-1}}, 0.39~\mathrm{gL^{-1}h^{-1}}$	E. coli	Glycerol	Trinh and Srienc, 2009 (ref. 14)
Growth decoupled					
1	Propionic acid	34.62 g L^{-1}	P. jensenii	Glycerol	Zhuge <i>et al.</i> , 2014 (ref. 19)
2	Alpha-ketoglutarate,	$11\mathrm{gL^{-1}}$	C. glutamicum	Xylose	Tenhaef <i>et al.</i> , 2021 (ref. 20)
	succinate		.	•	
3	Protocatechuate	$9.51~{ m gL^{-1}}$	C. glutamicum	Glucose then xylose	Labib <i>et al.</i> , 2021 (ref. 21)
4	Vanillin	$900 \mathrm{\ mg\ L}^{-1}$	E. coli	Ferulic acid	Lo et al., 2016 (ref. 22)
5	1,2-Indandiol	262 mg L^{-1}	Rhodococcus sp.	Glucose	Stafford <i>et al.</i> , 2002 (ref. 23)
9	Polyhydroxybutyrate	$1.4~{\rm g}~{\rm L}^{-1}$	E. coli	Rich and minimal media glucose	Bothfeld <i>et al.</i> , 2017 (ref. 24)
7	Fatty alcohol	$150~{ m mg}~{ m L}^{-1},0.03~{ m g}~{ m g}^{-1}$	E. coli	Glucose	Chubukov <i>et al.</i> , 2017 (ref. 25)
8	Linalool	$10.9~{ m g~L}^{-1}$, 5.1% yield	Pantoea ananatis	Glucose + YE	Nitta <i>et al.</i> , 2021 (ref. 26)
6	$Isobutanol^b$	$0.53~{ m g~L^{-1}}, 0.31~{ m C-mol~C-mol^{-1}}$	C. glutamicum	Hemicellulose fraction + YE	Lange et al., 2018 (ref. 27)
10	Proline	$142.4 \text{ g L}^{-1}, 2.9 \text{ g L}^{-1} \text{ h}^{-1}, 0.31 \text{ g g}^{-1}$	C. glutamicum	Rich TSB media	Liu et al., 2022 (ref. 28)
11	Itaconate	$47 \mathrm{~g~L^{-1}}, 0.86 \mathrm{~g~L^{-1}~h^{-1}}$	E. coli	Glucose	Harder et al., 2018 (ref. 29)
12	Gamma-aminobutyric acid	$614~{ m g~L^{-1}}, 40.94~{ m g~L^{-1}}~{ m h^{-1}}$	E. coli	Glucose + YE	Ke <i>et al.</i> , 2016 (ref. 30)
13	Alpha-hydroxy ketones	62–84% yield	E. coli	Pyruvate and benzaldehyde	Liang et al., 2020 (ref. 31)
14	Caprolactone	$126 \text{ mM}, 0.78 \text{ mol mol}^{-1}$	E. coli	Cyclohexanol	Xiong et al., 2021 (ref. 32)
Feedback loops					
1	Vanillin	$900~{ m mg~L^{-1}}$	E. coli	Ferulic acid	Lo et al., 2016 (ref. 22)
2	Naringenin	$523.7~\mathrm{mg~L^{-1}}$	E. coli	MOPS glucose, glycerol, potassium acetate, palmitic acid.	Zhou et al., 2021 (ref. 38)
		,		stearic acid	,
3	Gamma-aminobutyric	$45.6~{ m g~L^{-1}}, 0.4~{ m g~g^{-1}}$	C. glutamicum	Glycerol	Wei <i>et al.</i> , 2022 (ref. 39)
4	Salicylic acid	$520~{ m mg~L^{-1}}$	E. coli	M9 glucose + glycerol	Dinh and Prather, 2019 (ref. 40)
5	Itaconate ^b Lycopene	$1.4~{ m gL^{-1}}$ 150.9 mg L $^{-1}$	P. putida E. coli	Deconstructed lignin Glucose + YE + peptone	Elmore <i>et al.</i> , 2021 (ref. 41) Li <i>et al.</i> , 2020 (ref. 42)
				1	

Open Access Article. Published on 26 novembre 2022. Downloaded on 29/09/2024 14:09:24.

This article is licensed under a Creative Commons Attribution-NonCommercial 3.0 Unported Licence.

Table 1 (Contd.)

7 Insulated genetic genetic elements — conit solutions pads with logic genetic elements — conit solutions pads with logic genetic elements E. coli; S. acrevisiae, B. acrevisiae, B. acrevisiae, B. acrevisiae, B. acrevisiae, B. acrevisiae, B. acrevisiae — conit solution acid base with logic genetic elements E. coli; S. acrevisiae, B. acrevisiae, B. acrevisiae — cerevisiae, B. acrevisiae Pase without AA. Pag L ⁻¹ , 53.5 mg g ⁻¹ — coli in Glucose + SD-Leu + yeast nitrog base without AA. acrevisiae Pase without AA. acrevisiae Pase without AA. acrevisiae Pase without AA. acrevisiae Pad or SC-His with 2% glucose and branched AA. acrevisiae Pad or SC-His with 2% glucose and branched AA. acrevisiae Pad or SC-His with 2% glucose and branched AA. acrevisiae Pad or SC-His with 2% glucose and plucose acrevisiae Pad or SC-His with 2% glucose and glucose acreate Pad or SC-His with 2% glucose and glucose and glucose and glucose and glucose and cannot acreate Pad or SC-His with 2% glucose and cannot acreate 2 — laconate 2.0 g L ⁻¹ 2.3 g L		Product	TRY^a	Host	Media	Reference
Figure Coli, S. E. coli E. co	7	Insulated genetic landing pads with logic	I	E. coli	M9 glucose + thiamine and casamino acids	Park <i>et al.</i> , 2020 (ref. 44)
Sate Circuits Sate Circuits Sate Circuits	∞	Insulated genetic landing pads with logic	ı	E. coli, S. cerevisiae, B.	I	Jones et al., 2022 (ref. 45)
Isobutanol 8.49 g L $^{-1}$, 53.5 mg g $^{-1}$ S. cerevisiae Shikimic acid 6 g L $^{-1}$, 0.43 g $^{-1}$, 0.48 g L $^{-1}$ h $^{-1}$ S. cerevisiae Shikimic acid 4 g L $^{-1}$, 3.8–4.5% yield S. cerevisiae S. cerevisiae Staty acids Sweenergy yield M. thermoacetica Sweenergy yield M. thermoacetica Sweenergy yield M. thermoacetica E. colii PhA 295.7 mg L $^{-1}$, 19.3% yield per CDW P. putida and S. cerevisiae PhA Sweenergy yield PhA PhA Sweenergy yield PhA PhA Sweenergy yield PhA Ph	6	gare circuits <i>N-</i> Acetylglucosamine	$0.2~\mathrm{g~L^{-1}}$	tnetatotaomicron S. cerevisiae	Glucose + SD-Leu + yeast nitrogen	Lee et al., 2021 (ref. 48)
Lactic acid Shikimic acid $\frac{1}{35}$ g L $^{-1}$, 0.43 g L $^{-1}$, 0.48 g L $^{-1}$ h $^{-1}$ S. cerevisiae Shikimic acid $\frac{1}{4}$ g L $^{-1}$, 3.8–4.5% yield $\frac{1}{4}$ S. cerevisiae Staty acids $\frac{1}{4}$ S. $\frac{1}{2}$ S. $\frac{1}{2}$ S. cerevisiae and Y. lipolytica and Y. lipolytica b. $\frac{1}{2}$ S. $\frac{1}{2}$	10	Isobutanol	$8.49~{ m g~L}^{-1},53.5~{ m mg~g}^{-1}$	S. cerevisiae	YPD or SC-dropout medium with 2% olucose and branched AA	Zhao <i>et al.</i> , 2018 (ref. 50)
atty acids 38% energy yield and Y. lipolytica and Y. lipolytica and Y. lipolytica aconate 20 g L^{-1} E. coli E. coli E. coli E. coli E. coli DHA 295.7 mg L^{-1} , 19.3% yield per CDW P. putida and S. cerevisiae 1.32 g L^{-1} 48.5% yield per CDW P. putida and E. coli P. putida and E. coli E. L. h. A. S. S. yield per CDW, 0.83 g P. putida	11 12 13	Lactic acid Shikimic acid Nerolidol	$6~{ m g~L^{-1}}$, 0.43 ${ m g~g^{-1}}$, 0.48 ${ m g~L^{-1}~h^{-1}}$ 4 ${ m g~L^{-1}}$, 3.8–4.5% yield	S. cerevisiae E. coli S. cerevisiae	YPD or SC-His with 2% glucose Glucose minimal media Glucose, sucrose, glucose + ethanol	Zhao <i>et al.</i> , 2021 (ref. 51) Komera <i>et al.</i> , 2022 (ref. 52) Peng <i>et al.</i> , 2017 (ref. 55)
Fatty acids 38% energy yield M. thermoacetica and Y. lipolytica Itaconate 20 g L^{-1} E. coli E. coli PHA 295.7 mg L^{-1} , 19.3% yield per CDW P. putida and S. cerevisiae PHA 48.5% yield per CDW P. putida and E. coli PHA 48.5% yield per CDW P. putida	Media optimizati0	ū				
Itaconate 20 g L^{-1} $E. coli$ — — $E. coli$ — — $E. coli$ PHA $E. coli$ $E. coli$	1	Fatty acids	38% energy yield	M. thermoacetica and Y. lipolytica	CO ₂ , glucose and gluconate, acetate	Park <i>et al.</i> , 2019 (ref. 56)
PHA 295.7 mg L^{-1} , 19.3% yield per CDW P. putida and S. cerevisiae PHA 1.32 g L^{-1} PHA 48.5% yield per CDW P. putida and E. coli PHA 48.5% yield per CDW P. putida PHA $L^{-1}h^{-1}$ PHA PLIS g L^{-1} , 67% yield per CDW, 0.83 g P. putida	3 5	Itaconate —	$^{20}~{ m g}~{ m L}^{-1}$	E. coli E. coli	Glycerol and xylose Rich and minimal media	Lu <i>et al.</i> , 2021 (ref. 57) Moreb <i>et al.</i> , 2020 (ref. 58)
PHA 1.32 g L $^{-1}$ P. putida and E. coli PHA 48.5% yield per CDW P. putida PHA 41.5 g L $^{-1}$, 67% yield per CDW, 0.83 g P. putida $L^{-1}h^{-1}$	4	PHA	295.7 mg L^{-1} , 19.3% yield per CDW	P. putida and S. cerevisiae	Xylose and octanoate	Wei et al., 2022 (ref. 59)
PHA 48.5% yield per CDW P . putida P . putida P . PHA P .	5	РНА	$1.32~{ m g}{ m L}^{-1}$	P. putida and E.	Glucose or xylose minimal media	Zhu <i>et al.</i> , 2021 (ref. 60)
PHA 41.5 g L^{-1} , 67% yield per CDW, 0.83 g <i>P. putida</i> $L^{-1}h^{-1}$	4	РНА	48.5% yield per CDW	P. putida	E2 minimal media with glucose, fructose, glycerol, octanoate or decanoate	Huijberts <i>et al.</i> , 1992 (ref. 65)
	ro.	PHA	41.5 g L $^{-1}$, 67% yield per CDW, 0.83 g L $^{-1}h^{-1}$	P. putida	Glucose minimal media	Poblete-Castro et al., 2014 (ref. 66)

^a TRY – titer (T), rate (R) and yield (Y). ^b Commodity chemical has been commercialized. ^c AA – amino acid; CDW – cell dry weight; Gly – glycine; His – histidine; MAD – modified AD7; MOPS – 3-(N-morpholino) propanesulfonic acid; PHA – polyhydroxyalkanoate; SD – synthetic defined; Thr – threonine; TSB – tryptic soy broth; YE – yeast extract; PPD – yeast extract peptone dextrose.

improvements. The consilience of metabolic and host engineering approaches with the optimization of production medium will enable ideal growth-production ratios that are stable (and thus predictable) across scales.

Beyond metabolism

For sustainable industrial scale-up, microbial bioconversion goes beyond metabolic engineering. Computational fluid dynamic (CFD)-based models have been used to understand the trade-off in industrial-scale bioreactors (https://www.nrel.gov/ docs/fy21osti/78334.pdf) together with bioprocess models, which have been recently reviewed,77 to assess the aeration and other parameters that are currently bottlenecks for these bioconversion processes. Heavily engineered strains designed for high TRY may not achieve this due to the regulatory mechanisms involved with nutrient starvation, stress and tolerance response, which are not well understood in non-conventional, fairly new microbial hosts. The engineering process itself may alter or change the tolerance, e.g. ref. 78. Non-traditional strategies have been used for the strain engineering of ethanol-producing S. cerevisiae by the overexpression of key protein kinases associated with flocculation-associated stress tolerance.79 Alternatively, the intrinsic heterogeneity of phenotypes caused by small molecule messengers has been leveraged to generate strains that segregate the population into stem cells and production cells.80 For cholesterol-like molecule production, the membrane physiology and trafficking were engineered in E. coli.81 Currently, many of these approaches remain disconnected and are implemented in isolation from each other. Thus, combining these approaches with mainstream metabolic engineering and medium optimization will allow us to develop sophisticated strains with potentially highly predictable performance high-scale production environments.

Conclusion and future scope

In this review, we discussed relevant examples of GC and DC, synthetic control for dynamic control, impact of the medium formulations, and research advances that go beyond metabolism (Table 1). Although examples of multiple carbon substrates exist for DC approaches, thus far, GC approaches have been only tested for a single carbon source. Thus, it will be interesting to see how GC-engineered strains perform with a mixed carbon source or when cultivated using rich media such as plant biomass hydrolysate or other industrial waste to make the bioconversion more sustainable and carbon neutral. In addition to designing GC strategies for the co-utilization of substrates, mixed community culturing of GC strains that are hard wired for each of the carbon sources that exist in the rich medium stream is necessary. Another challenge is the real-time unbiased comparison of different types of computational algorithms used for strain optimization, where the question remains, do they converge onto similar solutions or do they favor certain beachhead metabolites? A broader suite of

methods should be tested rather than cherry picking the familiar ones. Common platform and digital resources are available, which provide details on the different methods that have been tested thus far and the respective success (TRY fold improvement) and failures to identify gaps that need to be tested further. Advancement in genome-wide editing approaches, miniaturization of production systems and combinatorial methods that integrate designs for pathway, host and production conditions is increasing to test and reach the ideal growth-production trade-off.

Author contributions

DB and AM conceived the study. DB wrote the first draft of the manuscript and prepared figures. AM reviewed and edited the final manuscript. All authors have read and approved the final version of this manuscript for publication.

Conflicts of interest

There are no conflicts to declare.

Acknowledgements

This perspective is dedicated to celebrating Prof. David G. Lynn's 70th birthday. Both DB and AM are funded by the Joint BioEnergy Institute (https://www.jbei.org) supported by the US Department of Energy, Office of Science, through contract DE-AC02-05CH11231 between Lawrence Berkeley National Laboratory (LBNL) and the US Department of Energy.

References

- 1 N. R. Baral, O. Kavvada, D. Mendez-Perez, A. Mukhopadhyay, T. S. Lee, B. A. Simmons and C. D. Scown, Energy Environ. Sci., 2019, 12, 807-824.
- 2 M. Wehrs, D. Tanjore, T. Eng, J. Lievense, T. R. Pray and A. Mukhopadhyay, Trends Microbiol., 2019, 27, 524-537.
- 3 S. S. Fong, A. P. Burgard, C. D. Herring, E. M. Knight, F. R. Blattner, C. D. Maranas and B. O. Palsson, Biotechnol. Bioeng., 2005, 91, 643-648.
- 4 H. Yim, R. Haselbeck, W. Niu, C. Pujol-Baxley, A. Burgard, J. Boldt, J. Khandurina, J. D. Trawick, R. E. Osterhout, R. Stephen, J. Estadilla, S. Teisan, H. B. Schreyer, S. Andrae, T. H. Yang, S. Y. Lee, M. J. Burk and S. Van Dien, Nat. Chem. Biol., 2011, 7, 445-452.
- 5 C. R. Shen, E. I. Lan, Y. Dekishima, A. Baez, K. M. Cho and J. C. Liao, Appl. Environ. Microbiol., 2011, 77, 2905-2915.
- 6 E. I. Lan and J. C. Liao, Proc. Natl. Acad. Sci. U. S. A., 2012, 109, 6018-6023.
- 7 H. M. Purdy, B. F. Pfleger and J. L. Reed, Metab. Eng., 2022, **69**, 87-97.
- 8 Y. Chen, J. Bao, I.-K. Kim, V. Siewers and J. Nielsen, Metab. Eng., 2014, 22, 104-109.
- 9 B.-J. Harder, K. Bettenbrock and S. Klamt, Metab. Eng., 2016, 38, 29-37.
- 10 A. von Kamp and S. Klamt, Nat. Commun., 2017, 8, 15956.

- 11 P. Schneider, A. von Kamp and S. Klamt, *PLoS Comput. Biol.*, 2020, **16**, e1008110.
- D. Banerjee, T. Eng, A. K. Lau, Y. Sasaki, B. Wang, Y. Chen, J.-P. Prahl, V. R. Singan, R. A. Herbert, Y. Liu, D. Tanjore, C. J. Petzold, J. D. Keasling and A. Mukhopadhyay, *Nat. Commun.*, 2020, 11, 5385.
- 13 J. M. Otero, D. Cimini, K. R. Patil, S. G. Poulsen, L. Olsson and J. Nielsen, *PLoS One*, 2013, **8**, e54144.
- 14 C. T. Trinh and F. Srienc, Appl. Environ. Microbiol., 2009, 75, 6696–6705.
- 15 E. Orsi, N. J. Claassens, P. I. Nikel and S. N. Lindner, *Nat. Commun.*, 2021, 12, 5295.
- 16 P. Schneider, R. Mahadevan and S. Klamt, *Biotechnol. J.*, 2021, **16**, e2100236.
- 17 A. Cros, G. Alfaro-Espinoza, A. De Maria, N. T. Wirth and P. I. Nikel, *Curr. Opin. Biotechnol.*, 2022, 74, 180–193.
- 18 J. Chen, Y. Wang, P. Zheng and J. Sun, *Trends Biotechnol.*, 2022, **40**, 773–776.
- 19 X. Zhuge, L. Liu, H. Shin, J. Li, G. Du and J. Chen, *Bioresour. Technol.*, 2014, **152**, 519–525.
- 20 N. Tenhaef, J. Kappelmann, A. Eich, M. Weiske, L. Brieß, C. Brüsseler, J. Marienhagen, W. Wiechert and S. Noack, *Biotechnol. J.*, 2021, 16, e2100043.
- 21 M. Labib, J. Görtz, C. Brüsseler, N. Kallscheuer, J. Gätgens, A. Jupke, J. Marienhagen and S. Noack, *Biotechnol. Bioeng.*, 2021, **118**, 4414–4427.
- 22 T.-M. Lo, S. H. Chng, W. S. Teo, H.-S. Cho and M. W. Chang, *Cell Syst.*, 2016, 3, 133–143.
- 23 D. E. Stafford, K. S. Yanagimachi, P. A. Lessard, S. K. Rijhwani, A. J. Sinskey and G. Stephanopoulos, *Proc. Natl. Acad. Sci. U. S. A.*, 2002, 99, 1801–1806.
- 24 W. Bothfeld, G. Kapov and K. E. J. Tyo, ACS Synth. Biol., 2017, 6, 1296–1304.
- 25 V. Chubukov, J. J. Desmarais, G. Wang, L. J. G. Chan, E. E. Baidoo, C. J. Petzold, J. D. Keasling and A. Mukhopadhyay, *npj Syst. Biol. Appl.*, 2017, 3, 16035.
- 26 N. Nitta, Y. Tajima, Y. Yamamoto, M. Moriya, A. Matsudaira, Y. Hoshino, Y. Nishio and Y. Usuda, *Microb. Cell Fact.*, 2021, 20, 54.
- 27 J. Lange, F. Müller, R. Takors and B. Blombach, *Microb. Biotechnol.*, 2018, **11**, 257–263.
- 28 J. Liu, M. Liu, T. Shi, G. Sun, N. Gao, X. Zhao, X. Guo, X. Ni, Q. Yuan, J. Feng, Z. Liu, Y. Guo, J. Chen, Y. Wang, P. Zheng and J. Sun, *Nat. Commun.*, 2022, 13, 891.
- 29 S. Zhang, Y. Fang, L. Zhu, H. Li, Z. Wang, Y. Li and X. Wang, Syst. Microbiol. Biomanuf., 2021, 1, 444–458.
- 30 B.-J. Harder, K. Bettenbrock and S. Klamt, *Biotechnol. Bioeng.*, 2018, **115**, 156–164.
- 31 C. Ke, X. Yang, H. Rao, W. Zeng, M. Hu, Y. Tao and J. Huang, *SpringerPlus*, 2016, 5, 591.
- 32 Y.-F. Liang, L.-T. Yan, Q. Yue, J.-K. Zhao, C.-Y. Luo, F. Gao, H. Li and W.-Y. Gao, *Sci. Rep.*, 2020, **10**, 15404.
- 33 J. Xiong, H. Chen, R. Liu, H. Yu, M. Zhuo, T. Zhou and S. Li, *Bioresour. Bioprocess.*, 2021, **8**, 32.
- 34 K. Raj, N. Venayak and R. Mahadevan, *Metab. Eng.*, 2020, **62**, 186–197.
- 35 F. Jacob and J. Monod, J. Mol. Biol., 1961, 3, 318-356.

- 36 A. Pickar-Oliver and C. A. Gersbach, *Nat. Rev. Mol. Cell Biol.*, 2019, 20, 490–507.
- 37 A. V. Anzalone, L. W. Koblan and D. R. Liu, *Nat. Biotechnol.*, 2020, **38**, 824–844.
- 38 S. Zhou, S.-F. Yuan, P. H. Nair, H. S. Alper, Y. Deng and J. Zhou, *Metab. Eng.*, 2021, **67**, 41–52.
- 39 L. Wei, J. Zhao, Y. Wang, J. Gao, M. Du, Y. Zhang, N. Xu, H. Du, J. Ju, O. Liu and J. Liu, *Metab. Eng.*, 2022, 69, 134–146.
- 40 C. V. Dinh and K. L. J. Prather, *Proc. Natl. Acad. Sci. U. S. A.*, 2019, **116**, 25562–25568.
- 41 J. R. Elmore, G. N. Dexter, D. Salvachúa, J. Martinez-Baird, E. A. Hatmaker, J. D. Huenemann, D. M. Klingeman, G. L. Peabody, D. J. Peterson, C. Singer, G. T. Beckham and A. M. Guss, *Nat. Commun.*, 2021, 12, 2261.
- 42 C. Li, X. Gao, X. Peng, J. Li, W. Bai, J. Zhong, M. He, K. Xu, Y. Wang and C. Li, *Microb. Cell Fact.*, 2020, **19**, 202.
- 43 C. J. Hartline and F. Zhang, ACS Synth. Biol., 2022, 11, 2247–2258.
- 44 Y. Park, A. Espah Borujeni, T. E. Gorochowski, J. Shin and C. A. Voigt, *Mol. Syst. Biol.*, 2020, **16**, e9584.
- 45 T. S. Jones, S. M. D. Oliveira, C. J. Myers, C. A. Voigt and D. Densmore, *Nat. Protoc.*, 2022, **17**, 1097–1113.
- 46 B. K. Verma, A. A. Mannan, F. Zhang and D. A. Oyarzún, ACS Synth. Biol., 2022, 11, 228–240.
- 47 Y. Boada, F. N. Santos-Navarro, J. Picó and A. Vignoni, *Front. Mol. Biosci.*, 2022, **9**, 801032.
- 48 S.-W. Lee, P. Rugbjerg and M. O. A. Sommer, *ACS Synth. Biol.*, 2021, **10**, 2842–2849.
- 49 Y. Teng, J. Zhang, T. Jiang, Y. Zou, X. Gong and Y. Yan, *Curr. Opin. Biotechnol.*, 2022, 75, 102696.
- 50 E. M. Zhao, Y. Zhang, J. Mehl, H. Park, M. A. Lalwani, J. E. Toettcher and J. L. Avalos, *Nature*, 2018, 555, 683–687.
- 51 E. M. Zhao, M. A. Lalwani, J.-M. Chen, P. Orillac, J. E. Toettcher and J. L. Avalos, *ACS Synth. Biol.*, 2021, **10**, 1143–1154.
- 52 I. Komera, C. Gao, L. Guo, G. Hu, X. Chen and L. Liu, Biotechnol. Biofuels Bioprod., 2022, 15, 13.
- 53 V. V. Reshetnikov, S. V. Smolskaya, S. G. Feoktistova and V. V. Verkhusha, *Trends Biotechnol.*, 2022, **40**, 858–874.
- 54 T. S. Moon, C. Lou, A. Tamsir, B. C. Stanton and C. A. Voigt, *Nature*, 2012, **491**, 249–253.
- 55 B. Peng, M. R. Plan, A. Carpenter, L. K. Nielsen andC. E. Vickers, *Biotechnol. Biofuels*, 2017, 10, 43.
- 56 J. O. Park, N. Liu, K. M. Holinski, D. F. Emerson, K. Qiao, B. M. Woolston, J. Xu, Z. Lazar, M. A. Islam, C. Vidoudez, P. R. Girguis and G. Stephanopoulos, *Nat. Metab.*, 2019, 1, 643–651.
- 57 K. W. Lu, C. T. Wang, H. Chang, R. S. Wang and C. R. Shen, Metab. Eng. Commun., 2021, 13, e00190.
- 58 E. A. Moreb, Z. Ye, J. P. Efromson, J. N. Hennigan, R. Menacho-Melgar and M. D. Lynch, ACS Synth. Biol., 2020, 9, 1483–1486.
- 59 Z. Wei, Y. Zhu, M. Ai, C. Liu and X. Jia, *Can. J. Chem. Eng.*, 2022, DOI: 10.1002/cjce.24751, article ASAP.
- 60 Y. Zhu, M. Ai and X. Jia, Front. Bioeng. Biotechnol., 2021, 9, 794331.

- 61 M. Mauri, J.-L. Gouzé, H. de Jong and E. Cinquemani, PLoS Comput. Biol., 2020, 16, e1007795.
- 62 H. Joshi, J. Isar, D. A. Jain, S. S. Badle, S. B. Dhoot and V. Rangaswamy, Appl. Biochem. Biotechnol., 2021, 193,
- 63 M. Wehrs, J. M. Gladden, Y. Liu, L. Platz, J.-P. Prahl, J. Moon, G. Papa, E. Sundstrom, G. M. Geiselman, D. Tanjore, J. D. Keasling, T. R. Pray, B. A. Simmons A. Mukhopadhyay, Green Chem., 2019, 21, 3394-3406.
- 64 Y. Sasaki, T. Eng, R. A. Herbert, J. Trinh, Y. Chen, A. Rodriguez, J. Gladden, B. A. Simmons, C. J. Petzold and A. Mukhopadhyay, Biotechnol. Biofuels, 2019, 12, 41.
- 65 G. N. Huijberts, G. Eggink, P. de Waard, G. W. Huisman and B. Witholt, Appl. Environ. Microbiol., 1992, 58, 536-544.
- 66 I. Poblete-Castro, A. L. Rodriguez, C. M. C. Lam and W. Kessler, J. Microbiol. Biotechnol., 2014, 24, 59-69.
- 67 L. F. Huergo and R. Dixon, Microbiol. Mol. Biol. Rev., 2015, 79, 419-435.
- 68 M. Wehrs, J.-P. Prahl, J. Moon, Y. Li, D. Tanjore, J. D. Keasling, T. Pray and A. Mukhopadhyay, Microb. Cell Fact., 2018, 17, 193.
- 69 M. G. Thompson, L. E. Valencia, J. M. Blake-Hedges, P. Cruz-Morales, A. E. Velasquez, A. N. Pearson, L. N. Sermeno, W. A. Sharpless, V. T. Benites, Y. Chen, E. E. K. Baidoo, C. J. Petzold, A. M. Deutschbauer and J. D. Keasling, Metab. Eng. Commun., 2019, 9, e00098.
- 70 M. G. Thompson, M. R. Incha, A. N. Pearson, M. Schmidt, W. A. Sharpless, C. B. Eiben, P. Cruz-Morales, J. M. Blake-Hedges, Y. Liu, C. A. Adams, R. W. Haushalter, R. N. Krishna, P. Lichtner, L. M. Blank, A. Mukhopadhyay,

- A. M. Deutschbauer, P. M. Shih and J. D. Keasling, Appl. Environ. Microbiol., 2020, 86, 21.
- 71 S. D. Doig, F. Baganz and G. J. Lye, in Basic Biotechnology, ed. C. Ratledge and B. Kristiansen, Cambridge University Press, 2006, pp. 289-306.
- 72 P. Rohe, D. Venkanna, B. Kleine, R. Freudl and M. Oldiges, Microb. Cell Fact., 2012, 11, 144.
- 73 V. Singh, S. Haque, R. Niwas, A. Srivastava, M. Pasupuleti and C. K. M. Tripathi, Front. Microb., 2016, 7, 2087.
- 74 L. F. Motta Dos Santos, F. Coutte, R. Ravallec, P. Dhulster, L. Tournier-Couturier and P. Jacques, Bioresour. Technol., 2016, 218, 944-952.
- 75 P. Biniarz, F. Coutte, F. Gancel and M. Łukaszewicz, Microb. Cell Fact., 2018, 17, 121.
- 76 K. Iwai, M. Wehrs, M. Garber, J. Sustarich, L. Washburn, Z. Costello, P. W. Kim, D. Ando, W. R. Gaillard, N. J. Hillson, P. D. Adams, A. Mukhopadhyay, H. Garcia Martin and A. K. Singh, Microsyst. Nanoeng., 2022, 8, 31.
- 77 G. Wang, C. Haringa, H. Noorman, J. Chu and Y. Zhuang, Trends Biotechnol., 2020, 38, 846-856.
- 78 J. Gao, Y. Li, W. Yu and Y. J. Zhou, Nat. Metab., 2022, 4, 932-
- 79 P.-L. Ye, X.-Q. Wang, B. Yuan, C.-G. Liu and X.-Q. Zhao, Bioresour. Technol., 2022, 348, 126758.
- 80 G. Bowman, M. Gomelsky and N. Mushnikov, Microbial Stem Cell Technology, US pat., 20190322980 A1, 2019.
- 81 M. C. Santoscoy and L. R. Jarboe, Metab. Eng., 2022, 73, 134-143.
- 82 X. Wang, E. E. K. Baidoo, R. Kakumanu, S. Xie, A. Mukhopadhyay and T. S. Lee, Biotechnol. Biofuels, 2022, 15, 137.